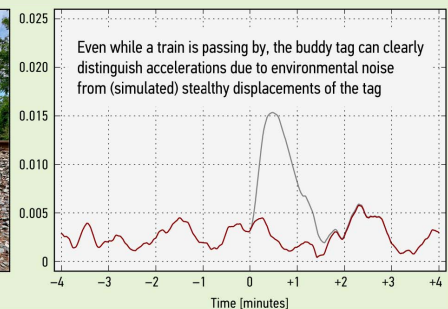
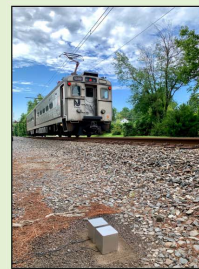


Verifying Deep Reductions in the Nuclear Arsenals: Development and Demonstration of a Motion-Detection Subsystem for a “Buddy Tag” Using Non-Export Controlled Accelerometers

Alexander Glaser¹ and Moritz Kütt²

Abstract—Future nuclear arms-control agreements may place numerical limits on items that are difficult to monitor with national technical means, even when complemented with onsite inspections. Such items could include small objects and mobile assets, such as non-deployed nuclear warheads and mobile missile launchers. Typically, this verification task can be addressed with unique identifiers, but standard tagging techniques may be unacceptable in this case due to host concerns about safety and intrusiveness. First proposed in the late 1980s and partially developed by Sandia National Laboratories in the early 1990s, the “Proximity Tag” or “Buddy Tag” concept seeks to overcome these concerns by separating the tag from the treaty accountable item itself. A buddy tag has two key elements: a tamper-indicating enclosure and a motion-detection system designed to detect illicit movements in a stand-down period. As part of this project, we have built a buddy-tag prototype for demonstration and evaluation purposes. This paper reviews the design choices and functionalities of the tag’s motion-detection subsystem. We pursue a modular approach for the tag’s hardware, built around an Arduino-class microcontroller and a non-export-controlled low-noise accelerometer, and use open-source algorithms for the motion-detection software. We discuss the results of an extensive experimental campaign involving both indoor and outdoor measurements assessing the performance of the tag under real-world environmental conditions.

Index Terms—Nuclear arms control, verification, tagging, motion detection, IIR filter.



I. BACKGROUND

FOR almost fifty years, the United States and Russia have successfully pursued nuclear arms control to manage the risks associated with their nuclear arsenals. These efforts are currently in an unprecedented crisis. In 2019, the Intermediate Nuclear Forces (INF) Treaty has fallen apart, and the New START Treaty may expire in 2021 without an extension

or immediate follow-on agreement. As a result, the world is likely to enter a period without bilateral nuclear arms control and, when it emerges, may have to face a number of new challenges, including some important ones related to verification of limits on nuclear stockpiles.

While both INF and START relied extensively on onsite inspections [1], [2], verification of future agreements may benefit from (or require) less intrusive types of inspections. There may also be separate arms-control agreements involving new partners such as China or North Korea, who are less familiar and probably also less comfortable with the concept of onsite inspections [3]. Finally, such agreements may place numerical limits on treaty-limited items (TLI) that are difficult to monitor with national technical means, even when complemented with onsite inspections [4]. Relevant TLI could include small objects, such as non-deployed nuclear warheads, which are impossible to account for with satellites; also, agreements may place more emphasis on mobile assets that are meant to be concealed, such as missile launchers deployed in remote,

Manuscript received December 29, 2019; revised February 14, 2020; accepted February 18, 2020. Date of publication March 5, 2020; date of current version June 4, 2020. This work was supported in part by the U.S. Department of State’s Bureau of Arms Control, Verification and Compliance (AVC), and in part by the U.S. Department of Energy’s Consortium for Verification Technology under Award DE-NA 0002534. The associate editor coordinating the review of this article and approving it for publication was Prof. Guiyun Tian. (Corresponding author: Alexander Glaser.)

Alexander Glaser is with the Department of Mechanical and Aerospace Engineering, Princeton University, Princeton, NJ 08542 USA (e-mail: alx@princeton.edu).

Moritz Kütt is with the Institute for Peace Research and Security Policy at the University of Hamburg, 20144 Hamburg, Germany.

Digital Object Identifier 10.1109/JSEN.2020.2978540



Fig. 1. North Korea's Hwasong 15 missile on its transporter erector launcher (TEL) in a photo released in November 2018. Confirming limits on such launchers would likely be a key part of a future arms-control or denuclearization agreement with North Korea. Source: Korean Central News Agency (KCNA).

forested areas (Figure 1). This will pose qualitatively new challenges for nuclear verification and may therefore also require new verification technologies.

In principle, all numerical limits can be confirmed by tagging TLI with unique identifiers, which effectively transforms such a numerical limit into a ban on untagged items [5], [6]. Verification can then primarily rely on inspection of randomly selected TLI and their tags.

Directly attaching physical tags can be difficult to implement in practice, however, because the monitored party may have safety or security concerns, and inspections would necessarily be highly intrusive.¹ Furthermore, the exact locations of mobile missile launchers (or non-deployed nuclear warheads) are generally considered highly sensitive information, which would further complicate access to these for verification purposes.

To address this dilemma, in this article, we revisit the so-called “proximity tag” or “buddy tag” concept first considered in the late 1980s [7] and then further explored at Sandia National Laboratories in the early 1990s as an option to confirm numerical limits on missile systems (Figure 2). Somewhat counterintuitively, the buddy tag is generally not attached to a TLI, it only must remain close to the item at all times. As discussed in more detail in the next section along with the basic concept of operations, the critical capability of the buddy tag is a motion-detection subsystem that is able to distinguish stealthy motion from all relevant types of environmental noise in a variety of locations throughout the life-cycle of the TLI. Low-noise, high-sensitivity accelerometers and an efficient filter design are the key elements to enable such an application. Building on a brief paper published in 1991 [8], the main objectives of this joint project between Princeton and Sandia National Laboratories has been to develop a buddy-tag

¹In general, a tag must be attached to a part of the treaty-limited item that cannot be easily removed or replaced without incurring costs that are comparable to the item itself; these parts tend to be among the most sensitive components of a weapons system, where inspector access would be particularly difficult.

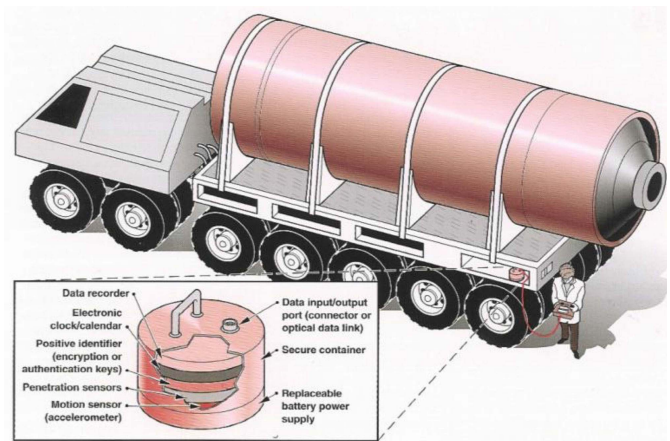


Fig. 2. Artist's conception of the buddy-tag concept supporting verification of limits on mobile missile launchers. Source: Jim Fuller via U.S. Department of Energy [9].

prototype using modern software and hardware concepts. We use non-export controlled, consumer-grade accelerometers. The choice of micro-electro-mechanical systems (MEMS) accelerometers allows for a much smaller prototype with reduced power consumption.² We offer new and reproducible results for the buddy-tag prototype and examine the viability and potential value of the concept for verifying future arms-control agreements.

II. BUDDY TAG CONCEPT OF OPERATIONS

Separating the tag from the item it is associated with (as opposed to a standard tag that is physically and securely attached to an item) is an unconventional concept; as a result, verification approaches using the buddy tag are also unconventional [10]. To facilitate the discussion, we use a nominal scenario, in which the total number of mobile missile launchers in the arsenal of a nuclear weapon state is limited by an arms-control agreement. The challenge is to gain confidence in the fact that no undeclared, additional launchers are deployed. In a tagging regime using buddy tags, a party would declare a certain number of mobile launchers and receive exactly one (unique and unclonable) tag for each. The monitored party would then co-locate these tags with the launchers. In this particular case, the tag could in principle be carried by the launchers themselves (Figure 2). Alternatively, the tag could be stored in a building at an accessible onsite location along with all other tags associated with the launchers in a particular deployment area. These deployment areas are large and geographically separate regions that are declared by the monitored party (but that are also easily identifiable via satellite). The basic idea is that, during a short-notice onsite inspection later on, the inspected party must be able to present one buddy tag for each launcher present in a particular deployment area. In practice, once an inspection is called, the selected site goes into immediate stand-down, and the monitored party promptly

²The original prototype of the motion-detection subsystem used three (export-controlled and ITAR-regulated) single-axis accelerometers using resonating-quartz technology primarily used for defense applications.

activates all buddy tags present at the site. The inspecting party may use reconnaissance satellites or other “national technical means” to monitor the site, especially, its exit routes.

Now, assume that the number of missile launchers in the deployment area exceeds the number of buddy tags that are available at the site, perhaps because the country has a number of undeclared additional launchers and sought to hide them “in plain sight” in the same area.³ If the monitoring party chooses this particular area for inspection, either by chance or based on intelligence, the inspected party has two options to evade detection: First, it could make an attempt to remove the undeclared launchers from the deployment area before the inspectors arrive; for all practical purposes, one can assume that this is not a viable strategy given the size of the launchers and given that the monitoring party would closely monitor the area. Second, the inspected party could seek to move buddy tags located at another site into the area. This is the most relevant evasion strategy, and the buddy-tag concept addresses this scenario with a dedicated motion-detection subsystem. Once the inspectors arrive at the site, they can first confirm the integrity and the status of the tags, in particular, that none of them has been moved since the inspection was called, say within the last 24–48 hours.⁴ Inspectors would then proceed to confirm that the number of buddy tags matches the number of launchers in the deployment area. If the tag is used as a class tag, only the total numbers need to match up as buddy tags are not associated with particular TLI.⁵

The next section describes in more detail the hardware choices and the discrimination algorithm for the tag’s motion-detection subsystem, followed by a discussion of the main experimental results obtained with this new prototype.

III. MOTION-DETECTION SUBSYSTEM

MEMS accelerometers have become widely available over the past decades [11]–[13], and noise levels have improved significantly over time [14]. In parallel, stability of bias and scale factor improved [15], [16]. There are numerous applications for MEMS accelerometers today: they include airbag deployment systems used in the automotive industry, modern cell phones and cameras [17], and many scientific applications, including earthquake detection [18]. MEMS devices have reached high-end tactical-grade for military applications [19]. Several applications seek to measure displacement using accelerometers [20], [21]. To do so, a double integration of the data with regard to time is necessary, but sensor noise and drift can quickly lead to large errors in such estimates [17], [19], [22]–[26]. The present use case is less demanding: only the fact that a displacement has occurred needs to be established,

but not its magnitude or direction. In particular, navigation capabilities of the device are unnecessary and also undesired for security reasons.

We stipulate that any displacement of an object by a significant distance, i.e., on the order of hundreds of meters, will at some point exceed an acceleration of several $10 \mu\text{g}$ along the path. For reference purposes, $10 \mu\text{g}$ has previously been found to be an “extremely small acceleration and it is representative of extremely stealthy illegal movement, beyond the capability of even national level assets” [8]. An object that has been uniformly accelerated with $10 \mu\text{g}$ for 5 minutes moves with a velocity of 3 cm/s. Given the size of a typical deployment area, which can be on the order of 100,000 km^2 , such a velocity and corresponding displacements can be considered insignificant.⁶ Overall, we consider the ability to detect accelerations on the order of 20–40 μg and the ability to reliably distinguish these from intrinsic, cultural, and environmental noise adequate as a performance target for the tag. Importantly, ambient environmental noise may vary from location to location, while false-alarm rates must remain extremely low under all circumstances. These requirements inform the choice of hardware and the design of the algorithm for the motion-detection subsystem.

A. Hardware: ADXL355 Accelerometer

The buddy-tag prototype developed as part of this project is based on the ADXL355 accelerometer, which is a three-axis, “ultralow noise and ultrastable offset” MEMS device with micromachined, fully differential sensing elements [27]. The ADXL355 is one of the lowest-noise commercially available sensors with a noise density of $25 \mu\text{g}/\sqrt{\text{Hz}}$, but still classified as Class C for seismic applications [18], [28]. The datasheet further specifies an offset repeatability of at most $\pm 3.5 \text{ mg}$, much higher than required for tactical-grade accelerometers [19]. The ADXL355 has been successfully used for a variety of applications, including for detection of large rotor vibrations [29], oscillation measurements on telescopes [30], for community earthquake detection [31], and for monitoring the structural health of buildings [32], [33].

The ADXL355 uses an internal (analog) low-pass filter and a 20-bit ADC operating at 1.024 MHz to digitize the filtered signal. Additional downstream digital filtering consists of a two-stage low-pass decimation filter. The first stage is fixed with a 4 kHz output data rate and a low-pass filter cutoff (50% reduction in output response) at about 1 kHz. A variable second stage decimation filter is used for lower output data rates to achieve suitable antialiasing. For our prototype, five ADXL355 units are mounted on a massive (4-inch diameter) steel plate (Figure 5, left, $m \approx 1.65 \text{ kg}$). The accelerometers work in parallel, add robustness against sensor malfunction, and generally reduce noise by a factor of $\sqrt{5} \approx 2.2$. We use a small custom PCB with an oscillator that acts as the master clock for all devices and provides an additional synchronization signal, i.e. have all five accelerometers digitize the data

³This is not an unreasonable assumption or scenario. Missile launchers need support facilities and setting up a parallel, unknown deployment area would be difficult and probably impossible to conceal over time.

⁴A buddy tag would also indicate that it has been operating for a minimum amount of time to confirm that it was activated promptly after the stand-down of the site took effect.

⁵The fact that buddy tags can serve as class tags is an important advantage of the concept. For example, in the case of unique tags that are directly attached to items, inspectors could learn over time sensitive operational details; they could also, for example, infer information about the reliability of particular items by observing how often they are found in repair or maintenance facilities. Class tags avoid this problem.

⁶For example, the 1991 START Treaty required that “a deployment area shall not exceed 125,000 square kilometers in size” [34, Article VI]; indeed, typical deployment areas in Russia are about 300–400 km along their edges and far apart from each other [35].

in parallel. The data readout from all accelerometers occurs sequentially from internal FIFO buffers in the ADXL355.⁷ The data is then processed in real-time by an Arduino-type microcontroller (Adafruit Feather M0) using an Atmel ARM Cortex-M0+ processor clocked at 48 MHz [36]. An optional OLED module displays numerical and graphical data for development and testing purposes. Even with this module continuously displaying real-time information about the status of the tag, which would be unnecessary for a deployed device, two 18650 lithium-ion batteries with a combined capacity of 4400 mAh can power the prototype for more than 60 hours.

B. Software: Data Processing and Filter Design

The viability of the buddy tag's motion-sensing subsystem depends on the ability to process the incoming accelerometer data in real-time and to discriminate noise and vibrations from accelerations caused by true displacements of the tag. To accomplish this task, the data is passed through a simple infinite impulse response (IIR) bandpass filter:

$$y(n) = b_0 x(n) + b_1 x(n-1) + b_2 x(n-2) - a_1 y(n-1) - a_2 y(n-2)$$

Here, x and y denote unfiltered (raw) and filtered values of the current (n) and the two previous ($n-1$, $n-2$) samples. The filter is applied several times by the algorithm, and x and y can represent accelerations, velocities, and positions. The lower and higher cutoff frequencies are $f_1 = 0.01$ Hz and $f_2 = 1$ Hz.⁸ The lower cutoff eliminates constant offsets (including gravity) and sensor drift, the higher cutoff eliminates noise, which is both undesired and not of interest. Variations of these cutoff values did not show any significant changes in the performance of the tag in detecting illicit displacements. The default sampling rate is $f_s = 7.8125$ Hz, which is obtained by decimation of the original output data rate of 4000 Hz. For development purposes and performance assessments, we also considered a higher sampling rate of $f_s^* = 15.625$ Hz. For the default sampling rate, the following filter coefficients are used for all results discussed below:

$$\{b_0, b_1, b_2\} = \{ 0.29603664, 0, -0.29603664 \}$$

$$\{a_0, a_1, a_2\} = \{ 1, -1.40311981, 0.40792671 \}$$

These are the only numerical parameters that become part of the algorithm, which determines the value of the discrimination function for a given sampling frequency. Figure 3 shows the frequency response of the IIR filter for these parameters.

The algorithm itself uses a sequence of data filtering and integration steps for each of the axes (Figure 4). At the beginning of each time step, raw acceleration data is acquired simultaneously from all five devices. The acceleration data is then filtered separately, and these filtered data are combined to determine a “best” (e.g. average) value for each axis. In the current implementation, the algorithm discards the lowest and the highest values reported from the five units, and uses a

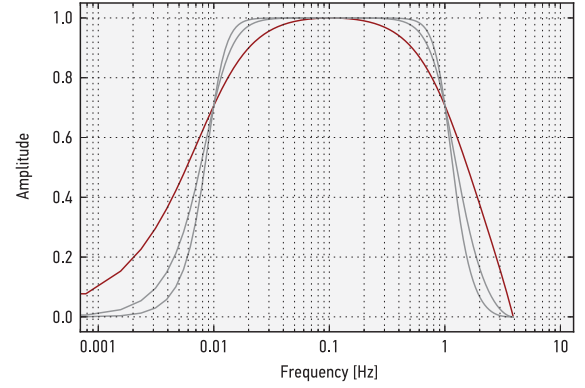


Fig. 3. Frequency response of the bandpass IIR filter implemented on the tag ($f_s = 7.8125$ Hz; $f_1 = 0.01$ Hz; $f_2 = 1$ Hz). While higher order filters offer better filtering characteristics, they result in oscillations of the filter response and the relevant observables, which is undesirable for this application. Buddy tag therefore uses the lowest order bandpass IIR filter (highlighted in red).

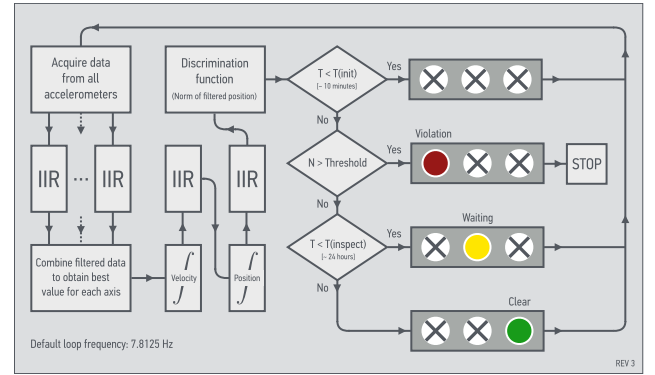


Fig. 4. Flow diagram of the buddy tag's algorithm. Raw data from all accelerometers are filtered and then combined to obtain one acceleration value for each axis. These values are integrated twice to obtain velocities and positions with filtering steps following each integration. The root-mean-square of the resulting three position values is an indicator for the displacement of the tag and used as the discrimination function (d). LEDs indicate the status of the tag depending on the time that has passed since activation and the value of d ; if d exceeds a threshold value after the filter has settled, the tag indicates a violation indefinitely, i.e., until the inspector arrives.

weighting scheme to average the remaining three values, giving the middle value a higher weight. The value obtained for the filtered acceleration, one for each axis, is then integrated to obtain a new velocity, which is filtered again to obtain filtered velocity. Finally, the filtered velocity is integrated to obtain a new displacement, which is filtered one last time to obtain filtered displacement. The three values obtained for the filtered displacement are then used to calculate the square root of the sum of the squares (d). This is the only number that will be used to determine if a violation has occurred, i.e., to determine if the tag has been moved or remains stationary.

The discrimination function has the units of displacement (m), but its value does not correspond to a meaningful physical distance given that the data has been filtered multiple times. As a result, the system is unable to estimate total displacement or direction of such a displacement. From a security perspective, this inability to navigate is considered

⁷The ADXL355 also includes a temperature sensor, and values are logged along with acceleration and timing data from all devices during measurements.

⁸The prototype proposed in [8] used similar cutoff values.

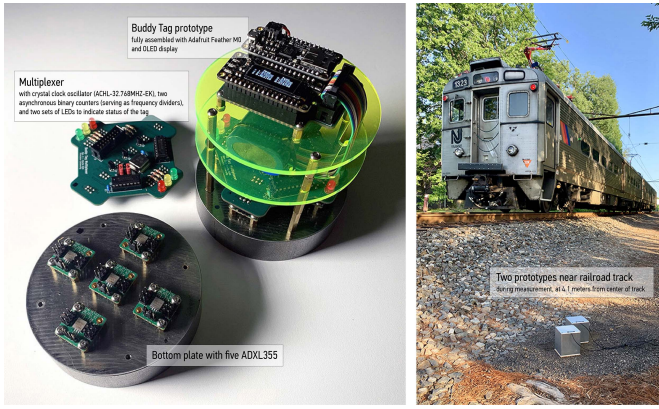


Fig. 5. Left: Components of the buddy-tag prototype. Five accelerometers are mounted on a steel ground plate. Data readout is synchronized and processed in real-time by an Arduino-type microcontroller. Right: Two buddy tags during measurements in July 2019 next to train tracks in Princeton, NJ. The tags are emplaced in aluminum enclosures to reduce environmental effects.

an advantageous feature of the concept. Moreover, for the default filter coefficients, the discrimination function will have “forgotten” previous displacements after 2–3 minutes; only LEDs or other types of electronic or physical indicators that are part of the tag show that a violation has occurred once the inspectors arrive at the scene.⁹

IV. EXPERIMENTAL RESULTS

The performance of the buddy-tag prototype has been studied in extensive indoor and outdoor measurement campaigns using two prototypes of the device. The overall objective of these measurements is to determine the capability of the tag to detect displacements while being robust against environmental and cultural noise.

It must be emphasized that it is beyond our capabilities to successfully displace the tag experimentally without triggering a clear and unambiguous response, i.e., without producing large values for the discrimination function (Figure 6). To assess the performance of the tag, we instead acquire data when the tag is at rest and then introduce artificial accelerations post-measurement, by adding offsets to the experimental data, to simulate a stealthy displacement of the tag.

A. Indoor Measurements

Indoor measurements have been carried out on a concrete floor in the basement of a residential building to determine the performance of the tag under favorable environmental conditions. These conditions could be representative for the use of the tag in a storage facility where noise levels would be minimal and predictable.

Figure 7 shows a slice of a typical dataset. The acceleration data acquired from the five ADXL355 units is first passed through the IIR filter to eliminate constant offsets, which are generally different for each axis and for each unit. The

⁹In principle, of course, the parties could agree on storing a log of the raw data acquired in the last 24–48 hours, which could be used to corroborate or challenge the outcome of an inspection.

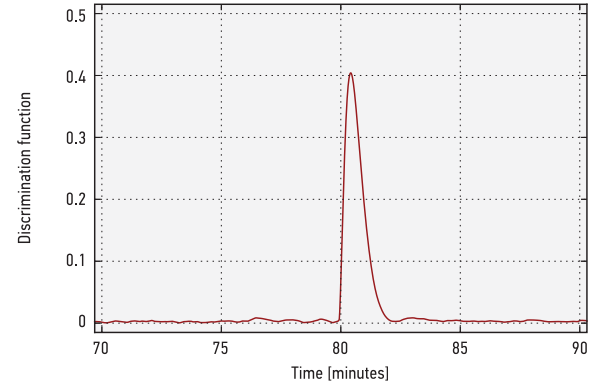


Fig. 6. Discrimination function as a function of time with a true millimeter-scale displacement attempt at about 80 minutes. It takes 2–3 minutes for the filter to fully recover from the disturbance, but the tag displays the violation indefinitely (Figure 4). Below, we will consider values of $d_T = 0.010$ – 0.015 as a clear indicator of a violation. Footage of the attempt is available in the online repository.

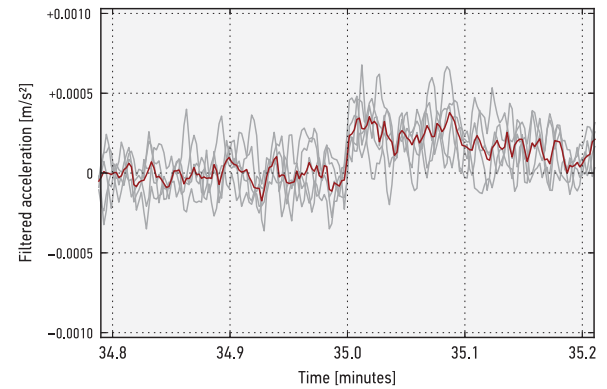


Fig. 7. Filtered acceleration data for one of the axes of the tag. Shown are the values reported by the individual accelerometers (gray) and the combined value based on the weighting/voting algorithm (red). At $t = 35$ minutes, a constant offset of $30 \mu\text{g}$ is artificially added to the data (post measurement) for an assessment of the system performance. Data acquired on concrete floor on July 15, 2019.

figure highlights the reduction in the noise level of the signal for one of the axes obtained by combining and averaging the data from different units. As an example, the figure also shows the effect of a sudden introduction of a constant acceleration of $30 \mu\text{g}$ along this axis. The step response of the IIR filter decays over time as the new offset becomes part of the prevailing constant offset for this particular axis. While $30 \mu\text{g}$ can be clearly distinguished in the filtered acceleration data, Figure 7 also suggests that one should not expect detection of stealthy accelerations that are, say, one magnitude smaller ($\sim 3 \mu\text{g}$) given the intrinsic noise levels of the ADXL355.

Figure 8 highlights the main results of the indoor measurements. In this case, the tag acquired data during an overnight measurement on a concrete floor, i.e., under favorable experimental conditions, to determine intrinsic limitations of the system. At rest, the value of the discrimination function does not exceed a value of $d = 0.005$ for the chosen filter design. In this example, artificial accelerations of 10 – $30 \mu\text{g}$ are introduced along one axis at $t = 35$ minutes, 40 minutes, and 45 minutes. While these offsets are clearly visible in the

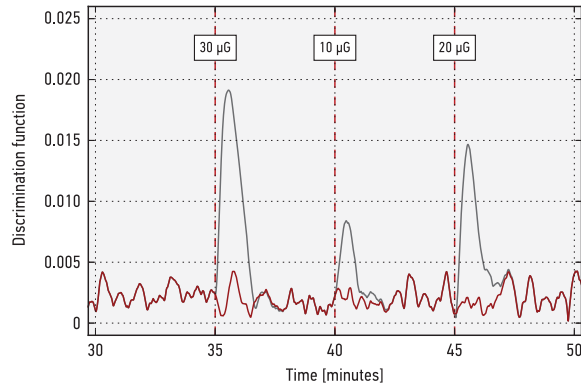


Fig. 8. Twenty minutes of data with three episodes of artificial accelerations at 35, 40, and 45 minutes (gray). These constant accelerations are added as offsets to the raw data, which is characterized by a finite background (red). All episodes are distinguishable against the noise. For this particular choice of filter coefficients, a suitable and conservative threshold value could be set at $d_T = 0.010$ – 0.015 ; this would enable detection of displacements in the 20–30 μg (but not in the 10 μg) range.

response of the discrimination function, the data also suggests that accelerations on the order of 10 μg may be too small to detect reliably under realistic field conditions encountered where higher noise levels ought to be expected. Based on these preliminary measurements, one could consider values in the 20–30 μg range as detectable; these would correspond to threshold values for the discrimination function of $d_T \approx 0.015$.

B. Outdoor Measurements

Building off of the indoor measurements, we carried out a series of outdoor experiments to assess the impact of realistic environmental conditions representative for an active military site. As laid out in the introduction, our main scenario is the use of the tag in a deployment area of mobile missile launchers, perhaps with the tags placed in a centrally located building, but in the presence of heavy vehicles that remain active even when the site is in a stand-down condition.

As a rather hard test case, we tested the performance of the tag immediately next to train tracks of the New Jersey Transit, Princeton Branch, where the tag is exposed to significant levels of vibrational noise from passing trains (Figure 5, right). The only train running on this branch—a train known as the “Dinky”—consists of two GE Arrow III railcars. Each car has a mass of 54,700 kg [37] for a total mass of the train of almost 110 tons, which is comparable to TELs that are used with heavy intercontinental ballistic missiles.¹⁰ The total length of the “Dinky” train is about 52 meters, and it passes the measurement location (+40.338460, −74.656425) at a speed of about 45 km/h. The distance of the tags from the center of the tracks was 4.1 meters. For all outdoor measurements, the tag was emplaced in an aluminum enclosure to minimize environmental effects, including rapid fluctuations in temper-

¹⁰For example, the currently largest TEL (MZKT-792210) used for the Russian Topol-M missile is a 16x16-wheeled 44-ton tractor with a maximum payload of 80 tons and a maximum total mass of 124 tons [38]. A TEL designed for shorter range missiles may have a total mass of 40–50 tons including the payload.

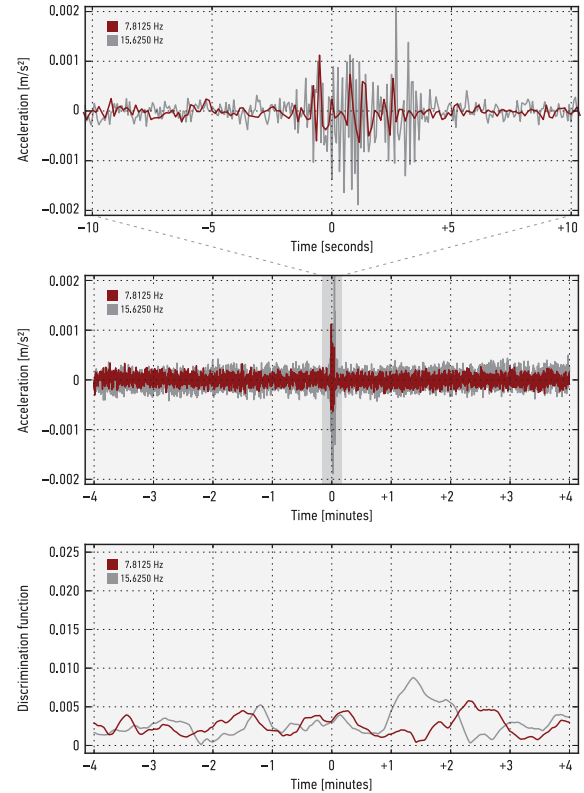


Fig. 9. Data acquired while train is passing the tag. Top and middle: Unfiltered acceleration data as recorded by the accelerometers; average values are shown without offset. Bottom: Response of the discrimination function, which is largely immune to the vibrational noise. For this particular event, a small but noticeable effect is visible (see discussion in text). The train passed the tag at 08h:13m:30s a.m. on July 25, 2019 ($t = 0$).

ature and humidity. A fieldable device would have to have a robust tamper-indicating enclosure.

Key results from the measurement campaign are shown in Figure 9. The strongest accelerations are observed along the axis perpendicular to the train track, but signals are also present along the other two axes, with the z-axis having the weakest signature. For a comparison of the ability of the IIR filter to eliminate high-frequency noise, we use two buddy-tag units that are operating with different sampling frequencies: in addition to the default frequency ($f_s = 7.8125$ Hz), data was also acquired with twice the frequency ($f_s^* = 15.625$ Hz). As expected, this data contains more vibrational noise than the data sampled with lower frequency, where the internal low-pass filter of the ADXL355 eliminates a larger fraction of the high-frequency components of the raw data. Note that the acceleration data shown in Figure 9 (top and middle) are not directly used by the algorithm; they are shown here primarily to illustrate that the accelerometers do pick up a clear signal from the passing train. As discussed above, the raw data is first passed through the bandpass IIR filter before being processed further.

The small but noticeable filter response one minute (for the higher sampling rate) and two minutes (for the lower sampling rate) after the train passed are most likely due to residual low-frequency components of vibrations caused by the train

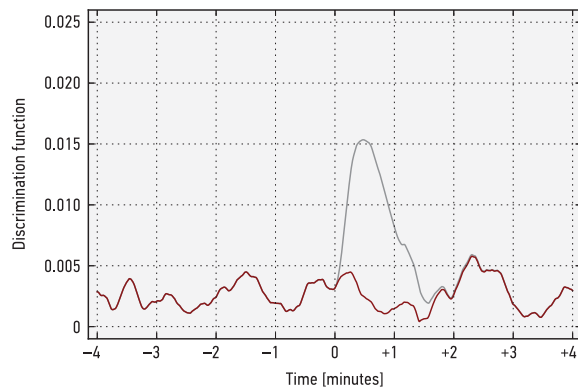


Fig. 10. Discrimination function combining data from train-track measurements with artificial acceleration offset. At the very moment when the train passes the tag (experimental data from Figure 9), $20 \mu\text{g}$ have been added post measurement to one of the axes to simulate a displacement attempt while the tag is experiencing strong vibrations. The response of the discrimination function is clearly visible and essentially equivalent to the results shown in Figure 8.

that are not eliminated by the filter. Similar effects were rarely observed in the experimental data; in the acquired datasets, about ten in total, the passing train had no unambiguous effect on the value of the discrimination function, which is an encouraging finding. Moreover, it must be emphasized that the scenario considered here, i.e., a train passing with high velocity at close distance, has to be considered an extreme one; a monitored party would make every effort to avoid similar circumstances in a situation where it seeks to demonstrate compliance with a treaty at a site or area that is in stand-down mode. Overall, the results shown in Figure 9 confirm that a threshold of $d_T \approx 0.015$ is viable even under unfavorable conditions that may be encountered in the field.

As a final test case, we combine the experimental data from the outdoor measurements with synthetic data to simulate artificial offsets. These results are shown in Figure 10. At the very moment when a train is passing the tag and disturbances are most pronounced (as also shown in Figure 9), we assume the adversary attempts a displacement of the tag with an acceleration of $20 \mu\text{g}$. The algorithm unambiguously detects such an attempt; in fact, the signal is just as pronounced as previously found under ideal conditions (shown in Figure 8).

V. CONCLUSION AND OUTLOOK

There are currently no established methods for an inspecting party to independently confirm a numerical limit on treaty limited items if the items themselves or their locations are highly sensitive in nature. In the case of mobile missile launchers, locations are particularly sensitive; in the case of nuclear warheads, attaching unique identifiers directly to these items may be considered unacceptable by the host. In both cases, inspections may also reveal sensitive operational information. The buddy-tag concept offers a radical solution to this dilemma by physically separating the treaty accountable item and its tag while retaining robustness.

As part of this project, we have developed a motion-detection subsystem of a buddy-tag prototype using modern software and hardware concepts and demonstrated

that such a tag can meet the requirements for relevant arms-control verification applications. For the first time, we offer reproducible results based on extensive measurement campaigns; the outdoor measurements, in particular, show that a discrimination algorithm using a series of IIR filtering steps can effectively eliminate environmental noise while remaining sensitive to extremely stealthy displacements of the tag.

The buddy-tag prototype described here offers a platform to demonstrate a wide range of relevant technologies without involving sensitive nuclear information. In particular, the buddy-tag concept can be used to develop and benchmark the performance of unique identifier technologies, tamper-indicating enclosures, secure electronics, and advanced algorithms for motion detection. Since the buddy-tag concept offers particularly simple and non-intrusive implementations, it might be appealing to a number of weapon states and could facilitate early consideration of a verification regime that tracks treaty-limited items. Taken together, the buddy-tag concept may therefore help chart a path toward multilateral nuclear arms-control and disarmament agreements.

ACKNOWLEDGMENT

The authors would like to thank S. DeLand, J. Brotz, and H. Smartt, who worked with us in the first phase of this project laying the basis for this follow-on effort, and S. Jordan who wrote the original paper on Sandia's Buddy Tag project in 1991. They would also like to thank B. Reimold, T. Schaffner, D. Steingart, M. Hepler, and A. Kim for their contributions to earlier prototypes of the tag. A. Glaser thanks J. Fuller for first mentioning the buddy-tag concept to him.

REFERENCES

- [1] J. P. Harahan, *On-Site Inspections Under the INF Treaty*, U.S. Dept. Defense, Washington, DC, USA, 1993.
- [2] E. Ifft, "Verifying the INF and START treaties," *AIP Conf. Proc.*, vol. 1596, no. 1, p. 8, 2014.
- [3] A. Glaser and Z. Mian, "Denuclearizing North Korea: A verified, phased approach," *Science*, vol. 361, no. 6406, pp. 981–983, Sep. 2018.
- [4] A. S. Krass, *Verification, How Much is Enough?* Lexington, MA, USA: Lexington Books, 1985.
- [5] T. Garwin, "Tagging systems for arms control verification," Anal. Assessment Corp., Sponsored Office Technol. Assessment, Washington, DC, USA, Tech. Rep. AAC-TR-10401/80, Feb. 1980.
- [6] S. Fetter and T. Garwin, "Using tags to monitor numerical limits," in *Technology and the Limitation of International Conflict*, Foreign Policy Institute, B. M. Blechman, Ed. Lanham, MD, USA: Johns Hopkins Univ., 1989.
- [7] S. D. Drell *et al.*, "Verification technology: Unclassified version," MITRE Corp., McLean, VA, USA, JASON Rep. JSR-89-100A, Oct. 1990.
- [8] S. E. Jordan, "Buddy Tag's motion sensing and analysis subsystem," Sandia Nat. Lab., Albuquerque, NM, USA, Tech. Rep. CONF-910774, 1991.
- [9] J. Fuller, "US START TID development program: The quest for extreme security unique identifiers (1986–1992)," Presentation, Apr. 2006.
- [10] J. Brotz, S. M. DeLand, A. Glaser, D. Steingart, and A. Kim, "Buddy tag CONOPS and requirements," Sandia Nat. Laboratories, Albuquerque, NM, USA, Tech. Rep. SAND2015-11143R, Nov. 2015.
- [11] L. M. Roylance and J. B. Angell, "A batch-fabricated silicon accelerometer," *IEEE Trans. Electron Devices*, vol. 26, no. 12, pp. 1911–1917, Dec. 1979.
- [12] N. Barbour, J. Elwell, and R. Setterlund, "Inertial instruments—Where to now?" in *Proc. Guid., Navigat. Control Conf.* Hilton Head Island, SC, USA: American Institute of Aeronautics and Astronautics, 1992, pp. 566–574.

- [13] J. Shieh, J. E. Huber, N. A. Fleck, and M. F. Ashby, "The selection of sensors," *Prog. Mater. Sci.*, vol. 46, nos. 3–4, pp. 461–504, 2001.
- [14] J. Chae, H. Kulah, and K. Najafi, "An in-plane high-sensitivity, low-noise micro-g silicon accelerometer with CMOS readout circuitry," *J. Microelectromech. Syst.*, vol. 13, no. 4, pp. 628–635, Aug. 2004.
- [15] N. Barbour and G. Schmidt, "Inertial sensor technology trends," *IEEE Sensors J.*, vol. 1, no. 4, pp. 332–339, 2001.
- [16] G. T. Schmidt, "GPS based navigation systems in difficult environments," *Gyroscopy Navigat.*, vol. 10, no. 2, pp. 41–53, May 2019.
- [17] F. Mohd-Yasin, D. J. Nagel, and C. E. Korman, "Noise in MEMS," *Meas. Sci. Technol.*, vol. 21, no. 1, 2010, Art. no. 012001.
- [18] J. Fu, Z. Li, H. Meng, J. Wang, and X. Shan, "Performance evaluation of low-cost seismic sensors for dense earthquake early warning: 2018–2019 field testing in Southwest China," *Sensors*, vol. 19, no. 9, p. 1999, Apr. 2019.
- [19] R. Bhardwaj, N. Kumar, and V. Kumar, "Errors in micro-electro-mechanical systems inertial measurement and a review on present practices of error modelling," *Trans. Inst. Meas. Control*, vol. 40, no. 9, pp. 2843–2854, Sep. 2017.
- [20] R. Ferrero, F. Gandino, and M. Hemmatpour, "Estimation of displacement for Internet of Things applications with Kalman filter," *Electronics*, vol. 8, no. 9, p. 985, Sep. 2019.
- [21] I. Chen, W. Hu, and R. Sun, "Displacement measurement algorithm using handheld device with accelerometer," in *Proc. Asia-Pacific Conf. Wearable Comput. Syst.*, 2010, pp. 122–126.
- [22] R. Ball and C. P. Lewis, "The effect of noise when deriving signals from accelerometers," *Meas. Control*, vol. 15, no. 2, pp. 59–61, Feb. 1982.
- [23] R. Liu, M. Liu, X. Sun, and Y. Wei, "Signal processing and accelerometer-based design for portable small displacement measurement device," in *Proc. Int. Conf. Embedded Softw. Syst.*, 2008, pp. 575–579.
- [24] S. Han, "Retrieving the time history of displacement from measured acceleration signal," *KSME Int. J.*, vol. 17, no. 2, pp. 197–206, Feb. 2003.
- [25] Y. K. Thong, M. S. Woolfson, J. A. Crowe, B. R. Hayes-Gill, and R. E. Challis, "Dependence of inertial measurements of distance on accelerometer noise," *Meas. Sci. Technol.*, vol. 13, no. 8, pp. 1163–1172, Jul. 2002.
- [26] A. Utz, C. Walk, A. Stanitzki, M. Mokhtari, M. Kraft, and R. Kokozinski, "A high-precision and high-bandwidth MEMS-based capacitive accelerometer," *IEEE Sensors J.*, vol. 18, no. 16, pp. 6533–6539, Aug. 2018.
- [27] *ADXL354/ADXL355: Low Noise, Low Drift, Low Power, 3-Axis MEMS Accelerometers, Data Sheet, Revision A*, Analog Devices, Norwood, MA, USA, 2018.
- [28] *Instrumentation Guidelines for the Advanced National Seismic System*, U.S. Geological Survey, Work. Group Instrum., Siting, Installation, Site Metadata Adv. Nat. Seismic Syst. (ANSS) Tech. Integr. Committee, Reston, VA, USA, Open-File Rep. 2008-1262, 2008.
- [29] I. Koene, R. Viitala, and P. Kuosmanen, "Internet of Things based monitoring of large rotor vibration with a microelectromechanical systems accelerometer," *IEEE Access*, vol. 7, pp. 92210–92219, 2019.
- [30] C. Kupfer, "Investigation and measurement of oscillations of the H.E.S.S. telescopes," M.S. thesis, Dept. Phys., Friedrich-Alexander-Universität Erlangen-Nürnberg, Erlangen, Germany, 2018.
- [31] J. Lee, J.-S. Kim, S. Choi, and Y.-W. Kwon, "A smart device using low-cost sensors to detect earthquakes," in *Proc. IEEE Int. Conf. Big Data Smart Comput. (BigComp)*, Feb. 2019, pp. 1–4.
- [32] S. Valenti *et al.*, "A low cost wireless sensor node for building monitoring," in *Proc. IEEE Workshop Environ., Energy, Structural Monitor. Syst. (EESMS)*, Jun. 2018, pp. 1–6.
- [33] S. González, J. C. Jiménez, R. Guevara, and I. Palacios, "IoT-based microseismic monitoring system for the evaluation of structural health in smart cities," in *Proc. Ibero-Amer. Congr. Smart Cities*, 2018, pp. 1–13.
- [34] *Treaty Between the United States of America and the Union of Socialist Soviet Republics on Further Reduction and Limitation of Strategic Offensive Arms (START I)*, Moscow, Russia, Jul. 1991.
- [35] P. Podvig, "Reducing the risk of an accidental launch," *Sci. Global Secur.*, vol. 14, nos. 2–3, pp. 75–115, Dec. 2006.
- [36] *Adafruit Feather M0 Adalogger*. Accessed: Mar. 11, 2020. [Online]. Available: <https://www.adafruit.com/product/2796>
- [37] B. Solomon, *Field Guide to Trains: Locomotives and Rolling Stock*. Stillwater, OK, USA: Voyageur Press, 2016.
- [38] *Truck Chassis MZKT-792210, Datasheet*, Minsk Wheel Tractor Plant (Volat), Minsk, Belarus. Accessed: Mar. 11, 2020. [Online]. Available: www.volatdefence.com/upload/iblock/cd9/792210_en_.pdf

Alexander Glaser received the Ph.D. degree in physics from TU Darmstadt, Germany. He is an Associate Professor with the Woodrow Wilson School of Public Affairs, and the Department of Mechanical and Aerospace Engineering, Princeton University. He co-directs the Program on Science and Global Security. Along with Harold Feiveson, Zia Mian, and Frank von Hippel, he is the coauthor of *Unmaking the Bomb* (MIT Press, 2014). For Princeton's work on nuclear warhead verification, Foreign Policy Magazine selected him as one of the 100 Leading Global Thinkers of 2014.

Moritz Kütt studied physics and political science. He received the Ph.D. degree in physics from TU Darmstadt in 2016, working on the role of Open Source Software for trust and transparency in nuclear arms control. He joined the research area Arms Control and Emerging Technologies at the Institute for Peace Research and Security Policy at the University of Hamburg (IFSH), in August 2019. Prior to his time in Hamburg, he has been multiple times at Princeton University's Program on Science and Global Security. First, he was a Visiting Student Research Collaborator from 2015 to 2016, funded through an ERP stipend by the German Academic Scholarship Foundation, and later as a Postdoctoral Research Associate from 2017 to 2019.